

Thalamic GABA levels and Occupational Manganese Neurotoxicity: Association with Exposure Levels and Brain MRI

Ruoyun E. Ma ^{a,b}, Eric J. Ward ^a, Chien-Lin Yeh ^{a,b}, Sandy Snyder ^{a,c}, Zaiyang Long^{a,d}, Fulya Gokalp Yavuz ^{e,f}
S. Elizabeth Zauber ^g, Ulrike Dydak ^{a,b,c}

a R.E. Ma, E.J. Ward, CL. Yeh, S. Snyder, U. Dydak.

School of Health Sciences, Purdue University, West Lafayette, IN, USA

b R.E. Ma, CL. Yeh, U. Dydak.

Department of Radiology and Imaging Sciences, Indiana University School of Medicine, Indianapolis, IN, USA

c S. Snyder, U. Dydak

Department of Speech, Language and Hearing Sciences, Purdue University, West Lafayette, IN, USA

d Z. Long

Department of Radiology, Mayo Clinic, Rochester, MN, USA

e F. Gokalp Yavuz

Department of Statistics, Purdue University, IN, USA

f F. Gokalp Yavuz

Yildiz Technical University, Istanbul, Turkey

g S.E. Zauber.

Department of Neurology, Indiana University School of Medicine, Indianapolis, IN, USA

Corresponding Author:

Ulrike Dydak, School of Health Sciences, 550 Stadium Mall Drive, West Lafayette, IN 47907

Tel.: 765.494.0550; Fax: 765.496.1377; udydak@purdue.edu

The authors have no financial conflicts of interests to declare and declare grants by NIH and CDC.

This is the author's manuscript of the article published in final edited form as:

Ma, R. E., Ward, E. J., Yeh, C.-L., Snyder, S., Long, Z., Yavuz, F. G., ... Dydak, U. (2017). Thalamic GABA levels and Occupational Manganese Neurotoxicity: Association with Exposure Levels and Brain MRI. *NeuroToxicology*. <https://doi.org/10.1016/j.neuro.2017.08.013>

Highlights:

- Elevated thalamic GABA levels were found in active welders using MRS
- Brain manganese deposition assessed by MRI was significantly higher in all welders
- The thalamic GABA levels were associated with Mn exposure and brain Mn deposition
- There appears to be an exposure threshold for effects on GABA and motor performance
- Only high-exposure welders showed significantly worse motor performance

Abstract:

Excessive occupational exposure to Manganese (Mn) has been associated with clinical symptoms resembling idiopathic Parkinson's disease (IPD), impairing cognitive and motor functions. Several studies point towards an involvement of the brain neurotransmitter system in Mn intoxication, which is hypothesized to be disturbed prior to onset of symptoms. Edited Magnetic Resonance Spectroscopy (MRS) offers the unique possibility to measure γ -amminobutyric acid (GABA) and other neurometabolites *in vivo* non-invasively in workers exposed to Mn. In addition, the property of Mn as Magnetic Resonance Imaging (MRI) contrast agent may be used to study Mn deposition in the human brain. In this study, using MRI, MRS, personal air sampling at the working place, work history questionnaires, and neurological assessment (UPDRS-III), the effects of chronic Mn exposure on the thalamic GABAergic system was studied in a group of welders ($N=39$) with exposure to Mn fumes in a typical occupational setting. Two subgroups of welders with different exposure levels (Low: $N = 26$; mean air Mn = 0.13 ± 0.1 mg/m³; High: $N = 13$; mean air Mn = 0.23 ± 0.18 mg/m³), as well as unexposed control workers ($N = 22$, mean air Mn = 0.002 ± 0.001 mg/m³) were recruited. The group of welders with higher exposure showed a significant increase of thalamic GABA levels by 45% ($p < 0.01$, $F(1,33) = 9.55$), as well as significantly worse performance in general motor function ($p < 0.01$, $F(1,33) = 11.35$). However, welders with lower exposure did not differ from the controls in GABA levels or motor performance. Further, in welders the thalamic GABA levels were best predicted by past-12-months exposure levels and were influenced by the Mn deposition in the substantia nigra and globus pallidus. Importantly, both thalamic GABA levels and motor function displayed a non-linear pattern of response to Mn exposure, suggesting a threshold effect.

Keywords: Manganese neurotoxicity, γ -aminobutyric acid (GABA), MRI, Magnetic Resonance Spectroscopy, thalamus, welding, rigidity

1. Introduction

Manganese (Mn) is an essential trace mineral for regulating human metabolism. In the central nervous system (CNS), Mn functions as a cofactor for several key enzymes (Aschner and Aschner ,2005; Aschner et al., 1992; Bouabid et al., 2016). Over-exposure to Mn in occupational settings may lead to neurotoxic effects affecting cognitive, psychiatric and motor functions, characterized as parkinsonian symptoms, and could develop into manganism in severe cases (Couper, 1837; Ellingsen et al., 2008; Guilarte and Chen, 2007; Klos et al, 2006; Lucchini 1995). Even with a relatively low level of exposure under or approaching the American Conference of Governmental Industrial Hygienists (ACGIH) Threshold Limit Value (TLV) before 2013 (0.2 mg/m³), subtle neuropsychological deficits were still observable (Roels et al., 2012; Bowler et al.,2011). In 2013, a ten-fold reduction of the ACGIH TLV for respirable Mn exposure levels was introduced. However, there has been a gap connecting individual Mn exposure levels with physiological changes to provide an assessment of a safe level of exposure below which no significant adverse physiological and behavioral effects would be of concern. A marker that may aid to establish such a connection is therefore desired.

Excessive exposure to Mn can cause a variety of effects on brain physiology. Animal studies have shown that the primary targets of Mn include the striatum and globus pallidus in the basal ganglia (Zheng et al., 1998). Mn overexposure has been associated with affecting dopamine (DA) neurotransmission in the striatum (Guilarte et al., 2008), enhancing oxidative stress and interfering with calcium and iron homeostasis in mitochondria in the basal ganglia (Tuschl et al., 2013), as well as abnormalities in glutamatergic and GABAergic transmissions (Racette et al., 2012), the primary excitatory and inhibitory projections within the basal ganglia neuronal pathways.

Gamma aminobutyric acid (GABA) plays a key role in mediating the direct and indirect pathway of the basal ganglia (Graybiel, 2000), both of which have GABAergic projections to the thalamus, which then propagate to cortical regions (Kropotova and Etlinger, 1999). The ganglia-thalamo-cortical pathway is mainly involved in voluntarily movement as well as in emotions, motivation and cognition that drive the movement (Everitt and Robbins, 2005, Haber and Calzavara, 2009). Despite the similarity in clinical manifestations between Mn-induced Parkinsonism and idiopathic Parkinson's disease (IPD), the mechanism and the affected structures in the basal ganglia are quite different (Olanow, 2004). Focusing on disruptions of the neurotransmitter system, animal studies have shown controversial conclusions as reviewed by Burton and Guilarte (2009), suggesting that the consequences of the disruption of the neurochemical system in the CNS due to Mn toxicity might depend on multiple factors including dose, length of exposure duration as well as how Mn is introduced to the CNS. Our previous study has found elevated thalamic GABA levels in a group of smelters with relatively high Mn exposure levels (Dydak et al, 2011). Moreover, the increase in GABA levels was found to be strongly associated with fine motor function (Long et al. 2014b). These results from relatively high exposure settings motivated the further investigation of the relation between individual Mn exposure levels and alterations of brain GABA levels, to advance the understanding of the mechanism of Mn neurotoxicity in the human brain and to test whether *in vivo* GABA levels may serve as marker of neurotoxic effects. Of particular interest is whether alterations in GABA levels due to Mn exposure also exist in a typical occupational setting in the US with individual respirable Mn air levels ranging from ~0.05 to 0.5 mg/m³.

One typical difference in Mn-induced parkinsonism as compared to IPD is the absence of resting tremor (Guilarte, 2010). In addition, kinetic tremor has been reported to be more common in Mn-induced parkinsonism compared to IPD (Cersosimo and Koller, 2005). Widespread rigidity appears to be one of the common symptoms shared by both, manganism and IPD (Standwood et al., 2009). The thalamus is known to be involved in both tremor and rigidity, but controlled by different neuronal pathways (Herrero MT et al., 2002). Tremor can be triggered by both basal ganglia and cerebellar input influencing thalamo-cortical interactions, while rigidity is considered to be more involved with basal ganglia and motor thalamus (Carr, 2002, Rodriguez-Oroz et al., 2009). Rigidity and tremor both have been widely studied in IPD cases (Bergman and Deuschi, 2002, Helmich et al., 2013, DeLong and Wichmann, 2007, Prochazka et al., 1997). However, the association between clinical rigidity and tremor and Mn-induced disruption of brain GABA has not been previously examined. Examining these associations could help

clarify mechanisms of Mn neurotoxicity, and perhaps help to distinguish these from the clinical characteristics of IPD.

Due to the paramagnetic properties of Mn, brain Mn deposition alters the longitudinal relaxation rate (R1) and thus the T1 ($=1/R1$) contrast measured by magnetic resonance imaging (MRI). R1 has been suggested to be linearly proportional to tissue Mn deposition in animal models with high exposures (Chuang et al., 2009, Fitakakis et al., 2006). As brain GABA levels may be detected non-invasively *in vivo* using MEGA-edited magnetic resonance spectroscopy (MRS) (Mullins et al., 2014), investigating the association between R1 values and GABA levels provides a direct and practical approach to study the effect of brain Mn levels on the GABAergic system.

A shortcoming of most neuroimaging studies on occupational Mn exposure is the lack of information on individual exposure to Mn. In some cases, a very crude approximation is made by simply using reported welding hours (e.g. Lee et al., 2015). In others exposure is estimated from models using information obtained through work history questionnaires (e.g. Racette et al., 2012). However, work settings constantly change and exposure levels are dependent on factors including metal type, enclosure and ventilation condition of the work space, time period, filter location, and perhaps other factors. (Hobson et al. 2011). The respirable fraction of airborne Mn, sampled from the air within the welding helmet, is expected to best represent individual exposure levels (Harris et al. 2005). According to literature reports, since 2000, the mean airborne Mn levels for various cohorts across the world spans a rather large range from 0.062 mg/m^3 to 0.49 mg/m^3 (Ellingsen et al. 2006, Pesch et al. 2012, Bowler et al. 2007, Smargiassi et al. 2000). Therefore, in this study personal air sampling at the working place was used, which should provide the most accurate information on individual exposure levels.

In this study, a group of Mn-exposed welders and matched control subjects without Mn exposure were recruited and examined using MRI, MRS, personal air sampling at the working place, work history questionnaires, and neurological assessment. The study aimed at investigating the response of *in vivo* GABA levels in thalamic and striatal brain regions, measured by MRS, to 1) individual Mn exposure levels, 2) R1 values measured by MRI and indicative of brain Mn deposition, and 3) motor performance, including tremor and rigidity, determined by the Unified Parkinson's Disease Rating Scale III (UPDRS III).

2. Material and Methods

2.1. Subject recruitment:

Male welders ($N=39$) and age-matched male control subjects ($N=22$) were recruited from a truck trailer manufacturer in the U.S. Welders had to be welding for at least 3 years at this factory to be eligible to participate. Control subjects were recruited from the same factory and had not been exposed to welding fumes (e.g. working in assembly lines). None of the subjects had any history of neurological or psychiatric disorder. The study was approved by the Institutional Review Board at Purdue University. Written informed consent forms were obtained from all subjects prior to the participation in the study. As it was noticed during the study that some welders had significantly higher individual exposure levels due to factors including higher airborne Mn exposure and more confined welding space, the welders were further grouped into two subgroups, noted as higher exposure group (HEX) and lower exposure group (LEX). The grouping was based on the recent exposure level of each subject represented by the past-3-months individual exposure level calculated by an exposure model further described in section 2.2. Welders with past-3-months exposure levels higher than $0.04 \text{ mg/m}^3\cdot\text{year}$ were grouped into the HEX subgroup, as shown in Fig. 1. This exposure level translates to an average *annual* exposure to an airborne Mn level of 0.16 mg/m^3 . All other welders were grouped into the LEX subgroup. Mean age, mean airborne Mn levels and years of welding of all subjects are listed in Table 1. As a first study of this population, the selected threshold was relatively arbitrary and initially informed by a clear difference in past-three-months exposure between subjects from the two plants of the factory tested. While the plant-defined difference with regard to worker exposures was not maintained over the course of recruitment due to wearing of respirators or other non-plant specific factors, this threshold nonetheless was maintained to separate the two subgroups.

All subjects visited a local imaging center for approximately four hours on a weekend day, where they were interviewed about their medical history, life habits (e.g. diet, smoking, drinking), and about their work history. Further, they performed a battery of motor and cognitive tests (this paper will only report on motor tests) and received an MRI scan of approximately 1 hour. Personal air sampling was performed on each subject during a full 8-hour shift at their work place on a weekday following their MRI exam.

2.2. Exposure Assessment:

An exposure model was developed to estimate each participant's cumulative exposure index (CEI) as an estimate of the individual cumulative respirable (<4 μm diameter) airborne Mn exposure for different time windows, which was derived from personal air samples as described below. For all subjects, high- and low-exposure, our sampling procedure used SKC aluminum cyclones with a cut-point of 4 μm , which collect the respirable particles capable of penetrating to the alveolar regions of the lungs as well as deposit in the brain via the olfactory pathway. Our sampling procedure was conceived primarily for measurements of direct personal exposure of welders, however as each subject was wearing the device for the length of his shift, also exposure to the ambient conditions present in the department was measured. Unpublished data on particle size distributions present in the ambient air at the factory, using an electrical low-pressure impactor (ELPI), showed that the ambient air at the factory typically contains less than ~10,000 particles/cm³ and that particle number concentrations were dominated by particles less than 2 μm in size (aerodynamic diameter). In contrast, exposure inside the welding helmet was extremely high (>1,000,000) particles/cm³, several orders of magnitude above ambient levels, and particles were small, ranging from 10nm-300nm. This shows that our sampling procedure is valid for both ambient and personal exposure. Furthermore, it shows that most exposure present for our cohort came directly from personal exposure to welding fume and not from ambient conditions. Therefore, the only difference between the HEX and LEX groups was the amount of direct personal exposure to welding fume.

The following exposure time windows were used in this study: exposure over the past three months (before the MRI measurement), exposure over the past year, and cumulative exposure over their working lifetime (back to age 18). For each case the CEI is calculated as a summation of the individual exposure from the current employer (CEI_{CE}), past employers (CEI_{PE}) and off the job welding (CEI_{OJ}) for the given exposure window in (mg/m³)·years as seen in equation 1 below (Ward et al. 2015).

$$\text{CEI (mg/m}^3\cdot\text{yr}) = \text{CEI}_{\text{CE}} + \text{CEI}_{\text{PE}} + \text{CEI}_{\text{OJ}} \quad [\text{Eq. 1}]$$

Our exposure model utilizes personal air sampling of respirable Mn, averaged to respirable Mn concentrations per department (working site within the factory). The average concentrations of respirable Mn were gathered from seventy-seven personal air samples with an average of six air samples per department to have accurate measures of exposure for each working site within the factory. Each personal air sample was collected over the duration of a full work shift (8 hours). The samples were collected inside the welding helmet for welders and on the shoulder in the personal breathing zone (PBZ) for control subjects. The CEI for the current employer is then calculated by summing over the measured average respirable Mn exposure for each department an individual has worked in during the respective time window, multiplied by the time worked at this department. For cumulative exposure including past employers or for off-the-job welding, the exposure model utilizes additional information from a detailed work history questionnaire, as well as weighting factors accounting for ventilation, welding frequency, welding type, base metals and use of respirator to better estimate the individual's exposure based on personal history (Laohaudomchok et al. 2011). These weighting factors were developed by Hobson et al. (2011) in a previous study investigating sixty-six other studies on how each of these factors changes Mn exposure. Overall, our exposure model gives estimates for the lifetime airborne respirable Mn exposure the individual may have had, as well as for respirable Mn exposure over the past three months and over the past year.

2.3. GABA MRS acquisition and analysis:

MRI and MRS exams were performed using a 3T GE Signa MRI scanner equipped with an 8-channel head coil. A high-resolution 3D T1-weighted FSPGR sequence (TR/TE=6.26/2.67 ms, resolution: $1\times1\times1$ mm 3) was followed by a fast T2-weighted sequence, acquiring sagittal and axial images aligned with the anterior and posterior commissure (AC/PC) for accurate placement of the MRS volumes of interest (VOIs). GABA spectra were acquired using the MEGA-PRESS sequence (TR/TE=2000/68 ms) (Mullins et al., 2014) with the editing pulses centered on 1.9 ppm (edit ON) and 7.5 ppm (edit OFF). 256 averages were acquired for edit ON and edit OFF spectra in an interleaved fashion. 8 averages of water reference scans without water suppression were acquired for frequency and phase correction. To determine the thalamic GABA level the MRS VOI was centered on the right thalamic region (25 mm \times 30 mm \times 25 mm) as shown in Fig. 2. The same GABA-edited MRS measurement was also performed on the right corpus striatal region (25 mm \times 30 mm \times 25 mm), which is referred

to as the striatal region in this paper, including globus pallidus and a part of putamen and caudate nucleus. This VOI intentionally overlapped partly with the thalamus VOI to detect or rule out a possible influence from striatal GABA signal to the large voxel size of the thalamic VOI.

Edit ON and OFF spectra were first post-processed with a Matlab 2013a (The MathWorks, Natick, 2013) tool to perform coil combination, zero and first order phase correction, as well as frame-by-frame spectral alignment. Difference spectra obtained from subtracting the averaged OFF spectra from the averaged ON spectra, showing a GABA peak at 3 ppm, were quantified using LCModel V6.3-1B (Provencher, 1993). A basis set generated by density matrix simulation using GABA coupling constants from Kaiser et al. (2008) was used. The examples of GABA-edited spectra from the thalamus and the striatum fitted by LCModel are shown in Fig. 2. 3D T1-weighted images were segmented into grey matter (GM), white matter (WM) and cerebrospinal fluid (CSF) using statistical parametric mapping (SPM8, Wellcome Department of Imaging Neuroscience, London, United Kingdom). The percentages of GM, WM and CSF for each VOI were then calculated from the tissue probability maps with a home-made Matlab (The MathWorks, Natick, MA) code. Since CSF has a near-zero concentration of GABA and other metabolites, GABA levels were corrected for CSF to obtain tissue GABA concentrations. Examples of tissue maps of GM, WM and CSF overlaid with the GABA VOIs are shown in Fig. 2. A widely-used approach in the MRS literature expressed by the following equation (Chowdhury et al., 2015) was applied to obtain the CSF-corrected tissue GABA levels from each VOI:

$$M_{cor} = (M_{raw}) \times \frac{35880 \times (f_{GM} + f_{WM}) + 55556 \times f_{CSF}}{35880} \times \frac{1}{1 - f_{CSF}} \quad [\text{Eq. 2}]$$

2.4. R1 ROI analysis:

Averaged R1 values for different brain regions were calculated based on T1 relaxation time maps. Whole brain 3D T1 relaxation time mapping was performed using the dual flip angle technique (Christensen et al., 1974) to assess brain Mn accumulation. Two spoiled gradient echo images (SPGR, TR/TE6.36/1.76 ms, bandwidth=224Hz/pixel, matrix dimension=256 x 192, resolution: 1x1x2 mm³) with flip angles 3° and 17 ° were

acquired. An inversion recovery sequence (IR-SPGR, TI=250ms) with the same parameters as the dual flip angle sequences was used to correct for inhomogeneity of the radiofrequency field (Deoni, 2007). T1 values were calculated for each pixel based on repetition time (TR), flip angle (α) and a factor that is proportional to the equilibrium longitudinal magnetization (ρ) using equation 3 (Sabati and Maudsley, 2013), with T1 maps generated by an in-house program in Matlab ():

$$S_{SPGR} = \frac{\rho(1-E_1)\sin\alpha}{1-E_1\cos\alpha}, \quad \text{where } E_1 = e^{-TR/T1} \quad [\text{Eq. 3}]$$

First, T1 values were measured for brain regions of interest (ROIs) in the globus pallidus, substantia nigra, caudate, and frontal cortex, which were reported to have high Mn deposition by Criswell et al. (2012). Circular ROIs with an area of 30 mm² were measured bilaterally on T1 maps, using the ROI tool in Matlab and Osirix (Pixmeo, Switzerland), as shown in Fig. 3. Second, R1 values of the above ROIs were calculated as the inverse T1 relaxation time. Finally, R1 values from left and right hemispheres were averaged for every brain structure.

2.5. Motor function examination:

Motor performance of the subjects was tested with the Unified Parkinson's Disease Rating Scale - Part III (UPDRS-III), which is a comprehensive evaluation of motor function used clinically to test severity of disease in patients with Parkinson Disease (Goetz et al, 2007). The examination was performed by a certified neurologist (S.E.Z.) for all subjects. Rigidity scores were calculated as the summation of 5 items: rigidity in the neck, rigidity in the left upper extremity (LUE), rigidity in the right upper extremity (RUE), rigidity in the left lower extremity (LLE) and rigidity in the right lower extremity (RLE). Tremor scores were calculated as the summation of 7 items: left and right kinetic tremor of the hands, rest tremor amplitude in lip/jaw, RUE, LUE, RLE and LLE. A higher UPDRS score indicates a worse motor performance. UPDRS scores up to 15 are considered within the normal range.

2.6. Statistical analysis:

Subjects were grouped into controls, welders from the HEX group, welders from the LEX group and all welders as a whole. Normality of each variable was tested using the Shapiro-Wilk test. All variables investigated were found to be normally distributed with p values from the Shapiro-Wilk test larger than 0.05. The differences of the measured variables between Mn-exposed groups and controls, as well as between welders in the HEX and LEX groups were examined using an analysis of variance (ANOVA) followed by Fisher's least significant difference (LSD) post hoc tests. A false discovery rate with q-value < 0.10 was used as a cutoff to control for multiple comparisons (Benjamini and Hochberg, 1995).

For correlation analysis, two hypotheses were tested: a) thalamic GABA levels are related to Mn exposure levels and to R1 values indicative of brain Mn deposition; b) motor function reflected by UPDRS total score, rigidity score and tremor score is related to thalamic and striatal GABA levels. For each hypothesis, pairwise Pearson correlation analysis was performed to test for correlations between all variables, followed by regression analysis with exhaustive model selection based on adjusted R-square. Type III sum of square (SS) for each dependent variable from the full models were calculated to examine the effect from each variable after considering all other variables. Highly correlated independent variables, such as past-3-months and past-12-months exposure levels, were not added to the same full model to avoid multicollinearity. For each independent variable in the final models the Variance Inflation Factor (VIF) was calculated to assess potential multicollinearity issues. A VIF below 2 indicates that the association with other dependent variables could be neglected in this study. No regression analysis was performed in controls due to the fact that their airborne exposure levels were close to or below the detection limit.

3. Results:

3.1. Group differences:

Table 2 presents the mean values and the standard deviation of 1) past-3-months, past-12-months and cumulative individual exposure levels, 2) GABA levels in the thalamus and striatum, 3) R1 values from the globus pallidus, substantia nigra, caudate nucleus and frontal cortex, 4) UPDRS total score, rigidity score and tremor score in all groups, as well as the p-values from group comparison tests. Respirable air Mn levels for welders ranged from 0.05 mg/m³ to 0.53 mg/m³. Welders had significantly higher exposure levels compared to the controls ($p<0.001$). Furthermore, the welders from the HEX group had significantly higher past-3-months, past-12-months ($p<0.001$) and cumulative ($p<0.05$) Mn exposure levels than welders from the LEX group.

Thalamic GABA levels were significantly elevated in HEX welders compared to the controls ($p<0.01$) and to LEX welders ($p<0.01$). However, there was no significant difference between LEX welders and controls. In some welders, a hyperintensity in the globus pallidus was observed in T1-weighted images (Fig. 5). For all welders, increased R1 values, indicating higher Mn deposition, were found in the globus pallidus ($p<0.01$), caudate nucleus ($p<0.05$) and frontal cortex ($p<0.01$) compared to control subjects. HEX welders had a higher R1 in the globus pallidus ($p<0.001$), substantia nigra ($p<0.05$), caudate nucleus ($p<0.05$) and frontal cortex ($p<0.01$). LEX welders only had a higher R1 in the globus pallidus ($p<0.01$) and frontal cortex ($p<0.001$). Differences in R1 values between the two welder subgroups were not significant.

UPDRS scores were significantly higher in HEX welders compared to the controls ($p<0.01$). No group difference in rigidity scores across groups was found. HEX welders had significantly higher tremor scores compared to LEX welders ($p<0.01$) and controls ($p<0.05$). It is worth noticing that all of our subjects had a rest tremor score of zero, indicating no rest tremor symptoms at all. Therefore, the tremor scores listed here are pure kinetic tremor scores.

Fig. 6 shows the main findings on GABA levels, exposure levels, R1 levels indicating brain Mn deposition, and motor function across the three groups.

3.2. Regression analysis:

The results of pairwise Pearson correlation analysis for each of the tested hypotheses are presented in Tables 3.1 and 3.2. Specifically, for the first hypothesis (thalamic GABA levels are related to Mn exposure levels and to R1 values indicative of brain Mn deposition), past-3-months and past-12-months exposure levels were highly correlated ($r = 0.77$, $p < 0.0001$). In addition, past-12-months exposure showed the most significant correlation with thalamic GABA, ($r = 0.47$, $p = 0.02$). The scatter plot for thalamic GABA levels and past-12-month exposure levels is shown in Fig. 6. The full model for this hypothesis hence only included the past-1-year exposure levels, cumulative exposure levels, R1 values from all of the 4 measured brain regions and age.

Although the inter-correlations between R1 values from all of the 4 brain regions were significant, these are most likely driven by Mn distributing throughout the brain in multiple brain regions and thus affecting R1 in all tested brain regions. A subject with more Mn exposure and higher R1 value in one brain region is likely to have higher brain R1 values across the brain. Therefore, the full regression model did not exclude R1 from any of the brain regions we measured. Age was added as an independent variable for each model because brain GABA levels have been reported to be related to age (Gao et al, 2013).

Tables 4.1 and 4.2 list the Type III SS of each variable from the full regression models on thalamic (table 4.1) and striatal (table 4.2) GABA, as well as their F and p values. The final model selected for the regression of the thalamic GABA levels on exposure levels and R1 values included past-12-months exposure levels, R1 from globus pallidus, R1 from substantia nigra and age as independent variables. The selected model for the regression of striatal GABA levels on exposure levels and R1 values included past-12-months exposure levels, R1 from frontal cortex, R1 from substantia nigra and age as independent variables. The results of the final models are listed in table 4.1 for thalamic GABA levels and in table 4.4 for striatal GABA levels.

This analysis reveals a statistically significant relation between thalamic GABA levels in welders and past-12-months exposure, R1 values from the globus pallidus, substantia nigra, and age. The VIF of all independent variables were below 2, indicating negligible multicollinearity. The striatal GABA levels were significantly related to R1 values from frontal cortex and substantia nigra, and to age. However, in this case the VIF of the R1 values from the two brain regions were higher than 2, indicating a potential multicollinearity issue. As can be seen from Table 4.2, only R1 values from the frontal cortex and age significantly ($p < 0.05$) improved model fitting.

For the second hypothesis (motor function reflected by UPDRS total score, rigidity score and tremor score is related to thalamic and striatal GABA levels), no significant correlation was found between thalamic GABA, striatal GABA and age by pairwise Pearson analysis (Table 3.2). Therefore, thalamic GABA, striatal GABA and age were all included in the full regression model. One type of motor function was examined at one time as the dependent variable. Thus, three regression analyses with model selection procedure were performed.

Statistical analyses results for the regression of UPDRS score on GABA and age are presented in Table 5.1 for Type III SS analysis and Table 5.2 for the final model summary. The p-values of independent variables indicate that only age is statistically significant in the final model. In addition, two separate regression models were conducted for rigidity score and tremor score, with statistical results presented in Tables 5.3 and 5.4, respectively. The results indicate a lack of any statistically significant relationship between GABA levels, age and rigidity score. Equally there is no significant relationship to tremor scores as indicated by the p-values listed in Table 5.4.

4. Discussion:

In this study, chronic increased exposure to Mn in an occupational setting is found to affect the GABAergic system. The significantly elevated thalamic GABA levels in Mn-exposed welders with relatively high exposure ($>0.04 \text{ mg/m}^3 \cdot \text{yr}$ over the past 3 months) confirm the results reported in earlier studies from Dydak et al. (2011)

and Long et al. (2014) conducted in China, but in a lower-exposure occupational setting than the previous studies. The fact that no difference was observed for the striatal VOI further confirmed that the signal change in GABA in the thalamic VOI came from the thalamus rather than from the part of the globus pallidus included in the thalamic VOI. In rodent studies alterations of GABA levels were observed in other brain regions such as the striatum (Gwiazda et al. 2002) and cerebellum (Lipe et al., 1999). However, studies on non-human primates yielded no change in brain GABA concentration under Mn exposure (Burton and Guilarte et al., 2009, Struve et al. 2007). These discrepancies suggest that the effects of Mn on the GABAergic system are complex. Species differences, length of exposure duration and delivery method could all play a role in the effect of Mn neurotoxicity. Furthermore, GABA levels were measured *ex vivo* in these animal studies, whereas all human MRS studies yield *in vivo* GABA levels, including signal from both synaptic and intracellular GABA.

In our study, welders with lower exposure, though with higher exposure level than controls, had similar GABA levels as controls. We therefore hypothesize that there could be a threshold level of individual Mn exposure that needs to be surpassed to cause a significant change in GABA levels in the thalamus. Pharmacokinetic studies on Mn modeling (Nong A. et al., 2008, Nong A. et al., 2009, Schroeter et al., 2011) suggested that Mn accumulation in tissue could be observed when inhaling Mn at exposure levels over 0.1 mg/m^3 . According to this pattern of the brain tissue's response to Mn exposure, it is reasonable that also a neurochemical alteration will only occur beyond a similar level of Mn exposure. According to the present study, extrapolating our arbitrary cut-off value between the two exposure groups of $0.04 \text{ mg/m}^3 \cdot \text{yr}$ over the past 3 months to an annual average, this threshold level might lie between 0.1 and $0.2 \text{ mg/m}^3 \cdot \text{yr}$ for annual Mn exposure. Follow-up studies to investigate a more accurate threshold of effect, and how the GABA levels change with the individual exposure longitudinally will be of high interest to provide further dynamic information and knowledge on how the GABAergic system responds to changes in Mn exposure individually.

The neuronal pathways in the basal ganglia and the thalamus, as illustrated in Fig. 7, reveal the interaction between the GABAergic and dopaminergic system. As reviewed by Guilarte (2010), the general findings on how Mn exposure affects the dopaminergic system suggest a decreased D2-receptor level in the striatum in the absence of change in D1-receptor levels and dopamine levels. The disinhibition of the indirect pathway is known to inhibit ongoing movement (DeLong and Wichmann, 2007). Thus, the elevation of GABA levels in the thalamus

rather than the striatum is in line with the above conclusions: since D2-receptors inhibit the indirect pathway (Neves et al. 2002), reduction in the number of striatal D2-receptors will cause stronger inhibition to the thalamus and thus higher thalamic GABA levels. However, further investigations are necessary to verify this hypothesis.

The results of the regression analysis of the GABA levels as response to individual exposure levels suggest that the increase of the thalamic GABA levels is most strongly dependent on the past-12-months Mn exposure. Our data further suggests that this response of thalamic GABA levels to individual Mn exposure over the past year may support the threshold theory: as seen in the scatterplot in Fig. 4, the higher exposed welders are driving this correlation, whereas LEX welders might not show much of a correlation with GABA at all. In comparison, life-time cumulative exposure levels did not seem to be associated with thalamic GABA levels. The reason could be that the establishment of a Mn equilibrium (Nong et al., 2008) in the brain is more dependent on the short-term exposure levels rather than life-long exposure levels. Though the half-life of Mn in human brain, especially the basal ganglia region has not been determined, Taketa et al. (1995) reported the Mn half-life between 51-74 days in rat brain tissue. In a study conducted by Erikson et al. (2007) on rhesus monkeys, excessive Mn deposition in the brain recovered to normal level 45-90 days after inhalation. This time frame agrees with our result of significant correlations between the thalamic GABA levels and short-term (past-12-months, past-3-months) exposure levels. The significant correlation between past-12-months exposure and thalamic GABA levels suggests that the effect of Mn on the neurochemical system could last somewhat longer in humans.

R1 values were found to be generally elevated in welders, indicating a larger amount of Mn deposition. Consistent with the sequential transport of Mn from striatum to pallidum-substantia nigra reported by Saleem et al. (2002), increased R1 values in the globus pallidus and substantia nigra were observed. The higher Mn deposition in frontal cortex found in welders is in line with rodent studies by Elder et al. (2006), which is likely to be a result of axonal transport of Mn from the striatum via the substantia nigra to the frontal cortex studied with manganese enhanced MRI (Paultre et al. 2003). Studies on Mn-exposed smelters by Long et al. (2014a) also demonstrated the vulnerability of frontal cortex to Mn exposure.

It is worth noting that there was no statistically significant difference in R1 values between HEX and LEX groups (globus pallidus: $p = 0.07$; caudate nucleus: $p = 0.40$; frontal cortex: $p = 0.90$; substantia nigra: $p = 0.09$). There was no correlation between exposure levels and R1 values from any of the investigated brain regions either as shown in Table 2.1. This suggests that although brain Mn accumulation after chronic exposure to Mn can be observed, the quantitative relationship between inhaled Mn and brain Mn is not straightforward. Mn transport into the CNS is a complex process which is known to involve crossing the blood brain barrier and choroid plexus, or intra-axonal uptake through olfactory nerve endings (Aschner et al., 2005; Yokel, 2009). Therefore, a more refined model including the bio-kinetic properties of Mn accumulation is suggested to be applied to better understand the relationship between brain Mn deposition and inhaled Mn levels.

In our study, the thalamic GABA levels were found to be significantly affected by Mn deposition in the substantia nigra. As shown in Fig. 7, the substantia nigra has GABAergic projections to the thalamus and dopaminergic projections to the striatum. Nigrostriatal dopaminergic neuronal pathways have been known to be affected by Mn neurotoxicity (Sloot and Gramsbergen, 1994; Erikson et al., 2005), while the effect on nigrothalamo pathways is not clear. Our result suggests that as one of the targets for excessive Mn deposition in the brain, the substantia nigra may be involved in the disruption of the GABAergic system by affecting the neuronal communication with the thalamus and further inhibiting thalamo-cortical projections. This would be in line with increased thalamic GABA levels, as well as increased hypokinetic symptoms such as rigidity. In addition, the R1 values in the globus pallidus also significantly, but negatively, predicted the thalamic GABA levels in welders. This negative correlation is not easy to explain with the same simplistic model of pathways as demonstrated in Fig.7 and will need further investigation.

The striatal GABA levels were significantly associated with Mn deposition in the frontal cortex. This could be explained by the direct projection from the frontal cortex to the striatum. As presented in the results, the correlation between the striatal GABA levels and R1 values from the substantia nigra is likely due to a multicollinearity issue. Thus, we do not suggest any association between Mn deposition in the substantia nigra and striatal GABA levels.

As a common clinical manifestation for IPD and manganism (Olanow, 2004), rigidity has been reported to be closely associated with the basal ganglia and the thalamus (Silkis, 2001). However, in our study, the level of

rigidity in the welders was not significantly different from controls. One possible reason could be that the exposure levels of the welders were not high enough to cause clinically observable adversity in rigidity. As clinical rating scale for a more severe movement dysfunction in Parkinson's disease, the UPDRS scale also might not be sensitive enough to pick up very subtle changes in motor dexterity. Another reason could be that the demand of fine movements in the welding process and frequent practice of such movements, which further requires a good coordination of various motor control centers in the brain, compensate the slightly increased rigidity, if there is any, in the welders (healthy worker effect).

The findings that no resting tremor was found in any subject and that only slightly but significantly more kinetic tremor was found in welders with higher exposure levels agree with the clinical reports on the symptoms of Mn-induced parkinsonism. However, our data does not suggest any direct association between GABA levels in the thalamus or striatum and the severity of tremor in Mn exposed subjects. One possibility is that the tremor levels of the welders recruited in this study were still in a normal range. The variation of the tremor scores were not directly controlled by GABA levels. In addition, the complexity of the mechanism of the tremor suggests that the basal ganglia are not the only brain areas associated with tremor. Therefore, such a regression analysis would over-simplify the association between GABA levels and tremor levels.

There are several limitations of this study. First, the effect of iron, which is another highly concentrated metal present in welding fume (Li et al., 2004), was not taken into account in this analysis. In most occupational exposure studies on Mn, co-exposure to iron has been ignored to date. However, the toxic effects of Mn on the CNS are known to be associated and interacting with iron due to their chemical similarities (Antonini et al., 2006). In this study, it is assumed that the reported findings were mostly related to Mn mainly because the iron exposure levels from the welders recruited for this study (mean (SD): 1.273 (0.522) mg/m³, ranging from 0.072 to 2.314 mg/m³) were much lower than the exposure limit of iron recommended by the ACGIH TLV (5 mg/m³). Another limitation is that the direct impact of Mn accumulation on neuronal pathways and connections, especially on the neuronal activities of the substantia nigra, could not be directly detected using the current techniques. Therefore, our interpretations of the correlation between Mn deposition in the substantia nigra and thalamic GABA levels will need verification with other methods in the future.

In summary, in our study, a significant elevation of GABA levels in the thalamus of Mn-exposed welders was observed. Importantly, this study suggests that the increase of thalamic GABA levels only occurs when the exposure level is higher than a certain threshold, which is likely around 0.1 mg/m³ respirable airborne Mn concentration. Furthermore, the elevated GABA levels were dependent both on past-12-months and past-3-months individual exposure levels, and directly associated with Mn deposition in the substantia nigra and the globus pallidus. Therefore, we suggest that the alteration of the thalamic GABA levels is a characteristic neurochemical response that links recent Mn exposure, as well as brain Mn deposition in the basal ganglia, to first effects on motor function. A next step is to test the reversibility of thalamic GABA levels when exposure to Mn is reduced, e.g. in compliance with the new ACGIH TLV of 0.02 mg/m³ airborne respirable Mn concentration.

Acknowledgments:

This study was supported by grants NIH/NIEHS R01 ES020529, CDC/NIOSH T03 OH008615 and by the Indiana Clinical and Translational Sciences Institute, funded in part by grant # RR 02576 from the National Institutes of Health, National Center for Research Resources. We thank Dr. Ralph Noeske for help with the GABA-editing sequence on the GE scanner, as well as Dr. James Murdoch for valuable discussions on GABA quantification. We also want to thank David Smigiel for useful discussions and help with the air sampling logistics.

References:

- Antonini JM, Santamaria AB, Jenkins NT, Albini E, Lucchini R. Fate of manganese associated with the inhalation of welding fumes: potential neurological effects. *Neurotoxicology* 2006;27(3):304-310.
- Aschner JL, Aschner M. Nutritional aspects of manganese homeostasis. *Mol Aspects Med* 2005; 26(4-5):353-362
- Aschner M, Erikson KM, Dorman DC. Manganese dosimetry: Species differences and implications for neurotoxicity. *Crit Rev Toxicol* 2005;35(1):1-32.
- Barbaccia ML, Africano D, Trabucchi M, Purdy RH, Colombo G, Agabio R, Gessa GL. Ethanol markedly increases "GABAergic" neurosteroids in alcohol-preferring rats. *Eur J Pharmacol* 1999;384 (2-3):R1-R2.
- Behar KL, Rothman DL, Petersen KF, Hooten M, Delaney R, Petroff OAC, Shulman GI, Navarro V, Petrakis IL, Charney DW, Krystal JH. Preliminary evidence of low cortical GABA levels in localized ¹H-MR spectra of alcohol-dependent and hepatic encephalopathy patients. *Am J Psychiatry* 1999;156(6):952-954.
- Benjamini Y, Hochberg Y. Controlling the false discovery rate: a practical and powerful approach to multiple testing. *J R Stat Soc* 1995;57(1):289-300.
- Berg D, Gerlach M, Youdim MBH, Double KL, Zecca L, Riederer P, Becker G. Brain iron pathways and their relevance to Parkinson's disease. *J Neurochem* 2001;79(2):225-236.

- Bergman H, Deuschl G. Pathophysiology of Parkinson's Disease: From clinical neurology to basic neuroscience and back. *Mov Disord* 2002;17 Supple 3 S28-S40.
- Bowler RM, Gocheva V, Harris M, Ngo L, Abdelouahab N, Wilkinson J, Doty RL, Park R, Roels HA. Prospective study on neurotoxic effects in manganese-exposed bridge construction welders. *Neurotoxicology* 2011;32(5):596-605.
- Bowler RM, Roels HA, Nakagawa S, Drezgic M, Diamond E, Park R, Koller W, Bowler RP, Mergler D, Bouchard M, Smith D, Gwiazda R, Doty RL. Dose-effect relationships between manganese exposure and neurological, neuropsychological and pulmonary function in confined space bridge welders. *Occup Environ Med*. 2007;64(3):167-177
- Bouabid S, Tinakoua A, Lakhdar-Ghazal, Benazzouz A. Manganese neurotoxicity: behavioral disorders associated with dysfunctions in the basal ganglia and neurochemical transmission. *J Neurochem* 2016;136:677-691.
- Burton NC, Guilarte TR. Manganese Neurotoxicity: Lessons learned from longitudinal studies in nonhuman primates. *Environ Health Perspect* 2009;117(3):325-332.
- Carr J. Tremor in Parkinson's disease. *Parkinsonism Rel Disord* 2002;8:223-234.
- Cersosimo MG, Koller WC. The diagnosis of manganese-induced parkinsonism. *Neurotoxicology* 2006;27(3):340-346.
- Chowdhury FA, O'Gorman RL, Nashef L, Elwes RD, Edden RA, Murdoch JB, Barker GJ, Richardson MP. Investigation of glutamine and GABA levels in patients with idiopathic generalized epilepsy using MEGAPRESS. *J Magn Reson Imaging* 2015;41(3):694-699.
- Christensen KA, Grand DM, Schulman EM, Walling C. Optimal determination of relaxation times of Fourier transform nuclear magnetic resonance. Determination of spin-lattice relaxation times in chemically polarized species. *J Phys Chem* 1974; 78: 1971–1977.
- Chuang KH, Koretsky AP, Sotak CH. Temporal changes in the T1 and T2 relaxation rates (ΔR_1 and ΔR_2) in the rat brain are consistent with tissue-clearance rates of elemental manganese. *Magn Reson Med* 2009;61:1528-1532.
- Couper J. On the effects of black oxide of manganese when inhaled into the lungs, British annals of medicine, pharmacy. *Vital Stat Gen Sci* 1837;1:41-42.
- Criswell SR, Perlmutter JS, Huang JL, Golchin N, Flores HP, Hobson A, Aschner M, Erikson KM, Checkoway H, Racette BA. Basal ganglia intensity indices and diffusion weighted imaging in manganese-exposed welders. *Occup Environ Med* 2012;69:437-443.
- Deoni SC. High-resolution T1 mapping of the brain at 3T with driven equilibrium single pulse observation of T1 with high-speed incorporation of RF field inhomogeneities (DESPOT1-HIFI). *J Magn Reson Imaging* 2007;26(4):1106-1111.
- Dydak U, Jiang YM,,Long LL, Zhu H, Chen J, Li WM, Edden RAE, Hu S, Fu X, Long Z, Mo XA, Meier D, Harezlak J, Aschner M, Morduch JB, Zheng W. In vivo measurement of brain GABA concentrations by magnetic resonance spectroscopy in smelters occupationally exposed to manganese. *Environ Health Persp* 2011;119(2):219-224.
- DeLong MR, Wichmann T. Circuits and circuit disorders of the basal ganglia. *Arch Neurol* 2007;64(1):20-24.
- Elder A, Gelein R, Silva V, Feikert T, Opanashuk L, Carter J, Potter R, Maynard A, Ito Y, Finkelstein J, Oberdörster G. Translocation of inhaled ultrafine manganese oxide particles to the central nervous system. *Environ Health Perspect* 2006;114(8):1172-1178.
- Ellingsen DG, Dubeikovskaya L, Dahl K, Chashchin M, Chashchin V, Zibarev E, Thomassen Y. Air exposure assessment and biological monitoring of manganese and other major welding fume components in welders. *J Environ Monit* 2006;8:1078-1086.
- Ellingsen DG, Konstantinov R, Bast-Pettersen R, Merkurjeva L, Chashchin M, Thomassen Y, Chashchin V. A neurobehavioral study of current and former welders exposed to manganese. *Neurotoxicology* 2008;29(1):48-59.
- Erikson KM, Dorman DC, Lash LH, Aschner M. Duration of airborne-manganese exposure in rhesus monkeys associated with brain regional changes in biomarkers of neurotoxicology. *Neurotoxicology* 2007;29(3):377-385.
- Erikson KM, Syversen T, Aschner JL, Aschner M. Interactions between excessive manganese exposures and dietary iron-deficiency in neurodegeneration. *Environ Toxicol Pharmacol* 2005;19(3):415-421.
- Everitt BJ, Robbins TW. Neural systems of reinforcement for drug addiction: from actions to habits to compulsion. *Nat Neurosci* 2005;8(11):1481–1489.

- Fitsanakis VA, Zhang N, Avison MJ, Gore JC, Aschner JL, Aschner M. The use of magnetic resonance imaging in the study of manganese neurotoxicity. *Neurotoxicology* 2006;27(5):798-806.
- Gao F, Edden RAE, Li M, Puts NAJ, Wang G, Liu C, Zhao B, Wang H, Bai X, Zhao C, Wang X, Barker PB. Edited magnetic resonance spectroscopy detects an age-related decline in brain GABA levels. *Neuroimage* 2013;78:78-52.
- Goetz CG, Fahn S, Martinez-Martin P, Poewe W, Sampaio C, Stebbins GT, Stern M.B, Tilley BC, Dodel R, Dubois B, Holloway R, Jankovic J, Kulisevsky J, Lang AE, Lees A, Leurgans S, LeWitt PA, Nyenhuis D, Olanow CW, Rascol O, Schrag A, Teresi JA, van Hilten JJ, LaPelle N. Movement Disorder Society-Sponsored Revision of the Unified Parkinson's Disease Rating Scale (MDS-UPDRS): Process, Format, and Clinimetric Testing Plan Movement Disorders. *Mov Disord* 2007;22(1):41-47.
- Guilarte TR. Manganese and Parkinson's disease: a critical review and new findings. *Environ Health Perspect* 2010;118(8):1071–1080.
- Guilarte TR, Burton NC, McGlothan JL, Verina T, Zhou Y, Alexander M. Impairment of nigrostriatal dopamine neurotransmission by manganese is mediated by pre-synaptic mechanism(s): Implications to manganese-induced parkinsonism. *J Neurochem* 2008;107(5):1236-1247.
- Guilarte TR, Chen MK. Manganese inhibits NMDA receptor channel function: implications to psychiatric and cognitive effects. *Neurotoxicology*.2007;28(6):1147-1152.
- Gwiazda RH, Lee D, Sheridan J, Smith DR. Sub-chronic low cumulative exposure to manganese affects striatal GABA but not dopamine. *Neurotoxicology* 2002;23(1):69–76.
- Haber S.N, Calzavara R. The cortico-basal ganglia integrative network: the role of the thalamus. *Brain Res Bull* 2009;78(2-3):69-74.
- Harris MK, Ewing WM, Longo W, DePasquale C, Mount MD, Hatfield R, Stapleton R. Manganese exposures during shielded metal arc welding (SMAW) in an enclosed space. *J Occup Environ Hyg*. 2005;2(8):375-382.
- Helmich RC, Toni I, Deuschl G, Bloem BR. The pathophysiology of essential tremor and parkinson's tremor. *Curr Neurol Neurosci Rep* 2013;13(9):378.
- Herrero MT, Barcia C, Navarro JM. Functional anatomy of thalamus and basal ganglia. *Childs Nerv Syst* 2002;18(8):386-404.
- Hobson A, Seixas N, Sterling D, Racette BA. Estimation of Particulate Mass and Manganese Exposure Levels among Welders. *Ann Occup Hyg* 2011;55(1):113–125.
- Jellinger KA. The role of iron in neurodegeneration: prospects for pharmacotherapy of Parkinson's disease. *Drugs Aging* 1999;14(2):115–140.
- Kaiser LG, Young K, Meyerhoff DJ, Mueller SG, Matson GB. A detailed analysis of localized J-difference GABA editing: theoretical and experimental study at 4 T. *NMR Biomed* 2008;21(1):22-32.
- Klos KJ, Chandler M, Kumar N, Ahlskog JE, Josephs KA. Neuropsychological profiles of manganese neurotoxicity. *Eur J Neurol* 2006;13(10):1139-1141.
- Kropotova JD, Etlinger SC. Selection of actions in the basal ganglia–thalamocortical circuits: review and model. *Int J Psychophysiol* 1999;31(3):197-217.
- Laohaudomchok W, Lin X, Herrick RF, et al. Toenail, Blood and Urine as Biomarkers of Manganese Exposure. *Journal of occupational and environmental medicine / American College of Occupational and Environmental Medicine*. 2011;53(5):506-510.
- Lee EY, Flynn MR, Du G, Lewis MM, Fry R, Herring AH, Van Buren E, Van Buren S, Smeester L, Kong L, Yang Q, Mailman RB, Huang X. T1 relaxation rate (R1) indicates nonlinear Mn accumulation in brain tissue of welders with low-level exposure. *Toxicol Sci* 2015;146(2):281-289.
- Li GJ, Zhang LL, Lu L, Wu P, Zheng W. Occupational exposure to welding fume among welders: alterations of manganese, iron, zinc, copper, and lead in body fluids and the oxidative stress status. *J Occup Environ Med* 2004;46(3):241-248.
- Lipe GW, Duhart H, Newport GD, Slikker W, Ali S. Effect of manganese on the concentration of amino acids in different regions of the rat brain. *J Environ Sci Health B* 1999;34(1):119-132.
- Long Z, Jiang YM, Li XR, Fadel W, Xu J, Yeh CL, Long LL, Luo HL, Harezlak J, Murdoch JB, Zheng W, Dydak U. Vulnerability of welders to manganese exposure – A neuroimaging study. *Neurotoxicology* 2014a;45:285-292.
- Long Z, Li XR, Xu J, Edden RAE, Qin WP, Long LL, Murdoch JB, Zheng W, Jiang YM, Dydak U. Thalamic GABA predicts fine motor performance in manganese-exposed smelter workers. *PLoS One* 2014b;9(2):e88220.

- Lucchini R, Selis L, Folli D, Apostoli P, Mutti A, Vanoni O, Iregren A, Alessio L. Neurobehavioral effects of manganese in workers from a ferroalloy plant after temporary cessation of exposure. *Scand J Work Environ Health* 1995;21(2):143-149.
- Mullins PG, McGonigle DJ, O'Gorman RL, Puts NAJ, Vidyasagar R, Evans CJ, Edden RAE. Current practice in the use of MEGA-PRESS spectroscopy for the detection of GABA. *Neuroimage* 2014;86(1):43-52.
- Neves SR, Ram PT, Iyengar R. G protein pathways. *Sci* 2002;296 (5573):1636–1639.
- Nong A, Teeguarden JG, Clewell III HJ, Dorman DC, Andersen ME. Pharmacokinetic modeling of manganese in the rat IV: Assessing factors that contribute to brain accumulation during inhalation exposure. *J Toxicol Environ Health A* 2008;71(7):413–426.
- Nong A, Taylor MD, Clewell HJ, Dorman DC, Andersen ME. Manganese tissue dosimetry in rats and monkeys: Accounting for dietary and inhaled Mn with physiologically based pharmacokinetic modeling. *Toxicol Sci* 2009;108(1):22–34.
- Olanow CW. Manganese-Induced Parkinsonism and Parkinson's disease. *Ann N.Y. Acad Sci* 2004;1012: 209–223.
- Paulter RG., Mongeau R., Jacobs RE. In vivo trans-synaptic tract tracing from the murine striatum and amygdala utilizing manganese enhanced MRI (MEMRI). *Magn Reson Med* 2003;50:33-39.
- Pesch B, Weiss T, Kendzia B, Henry J, Lehnert M, Lotz A, Heinze E, Käfferlein HU, Gelder RV, Berges M, Hahn JU, Mattenklott M, Punkenburg E, Hartwig A, Brüning T, The Weldox Group. Levels and predictors of airborne and internal exposure to manganese and iron among welders. *J Expo Sci Environ Epidemiol*. 2012;22:291-298.
- Prochazka A, Bennett DJ, Stephens MJ, Patrick SK, Sears-Duru R, Roberts T, Jhamandas JH. Measurement of rigidity in Parkinson's disease. *Mov Disord* 1997;12(1):24-32.
- Provencher SW. Estimation of metabolite concentrations from localized *in vivo* proton NMR spectra. *Magn Reson Med* 1993;30(6):672-679.
- Racette BA, Aschner M, Guilarte TR, Dydak, U, Criswell SR, Zheng, W. Pathophysiology of manganese-associated neurotoxicity. *Neurotoxicology* 2012;33(4):881–886.
- Racette BA, Criswell SR, Lundin JI, Hobson A, Seixas N, Kotzbauer PT, Evanoff BA, Perlmutter JS, Zhang J, Sheppard L, Checkoway H. Increased risk of parkinsonism associated with welding exposure. *Neurotoxicology* 2012;33(5):1356-1361.
- Rodriguez-Oroz MC, Jahanshahi M, Krack P, Litvan I, Macias R, Bezard E, Obeso JA. Initial clinical manifestations of Parkinson's disease: features and pathophysiological mechanisms. *Lancet Neurol* 2009;8(12):1128-1139.
- Roels HA, Bowler RM, Kim Y, Henn BC, Mergler D, Hoet P, Gocheva V.V, Bellinger DC, Wright R.O, Harris MG, Chang Y, Bouchard MF, Riojas-Rodriguez H, Menezes-Filho JA, Tellez-Rojo MM. Manganese exposure and cognitive deficits: a growing concern for manganese neurotoxicity. *Neurotoxicology* 2012;33(4):872-800.
- Sabati M, Maudsley AA. Fast and high-resolution quantitative mapping of tissue water content with full brain coverage for clinically-driven studies. *Magn Reson Imaging* 2013;31(10):1752-1759.
- Saleem KW, Pauls JM, Augath M, Trinath T, Prause BA, Hashikawa T, Logothetis NK. Magnetic resonance imaging of neuronal connections in the macaque monkey. *Neuron* 2002;34(5):685-700.
- Schroeter JD, Nong A, Yoon M, Taylor MD, Dorman DC, Andersen ME, Clewell HJ 3rd. Analysis of manganese tracer himetics and target tissue dosimetry in monkeys and humans with multi-route physiologically based pharmacokinetic models. *Toxicol Sci* 2011;120(2):481-498.
- Silkis I. The cortico-basal ganglia-thalamocortical circuit with synaptic plasticity. II. Mechanism of synergistic modulation of thalamic activity via the direct and indirect pathways through the basal ganglia. *Biosystems* 2001;59(1):7-14.
- Sloot WN, Gramsbergen JB. Axonal transport of manganese and its relevance to selective neurotoxicity in the rat basal ganglia. *Brain Res.* 1994;657:124-132.
- Smargiassi A, Baldwin M, Savard S, Kennedy G, Mergler D, Zayed J. Assessment of Exposure to manganese in welding operations during the assembly of heavy excavation machinery accessories. *Appl Occup Environ Hyg* 2000;15(10):746-750.
- Stanwood GD, Leitch DB, Savchenko V, Wu J, Fitsanakis VA, Anderson DJ, Stankowski JN, Aschner M, McLaughlin B. Manganese exposure is cytotoxic and alters dopaminergic and GABAergic neurons within the basal ganglia. *J Neurochem* 2009;110(1): 378-389.

- Struve MF, McManus BE, Wong BA, Dorman DC. Basal ganglia neurotransmitter concentrations in rhesus monkey following subchronic manganese sulfate inhalation. *Am J Ind Med* 2007;50(10):772-778.
- Takeda A, Sawashita J, Okada S. Biological half-lives of zinc and manganese in rat brain. *Brain Res* 1995;695(1):53-58.
- Tuschl K, Mills PB, Clayton PT. Manganese and the brain. *Int Rev Neurobiol* 2013;110:277-312.
- Ward E, Nour M, Snyder S, Rosenthal F, Dydak U. Human Toenails – A Viable Biomarker for Mixed Metal Exposure in UW Welders. *Toxicol Sci suppl.* 2015;144(1):347.
- Yokel RA. Manganese flux across the blood-brain barrier. *Neuromolecular Med* 2009;11(4):297-310.
- Zheng W, Ren S, Graziano JH. Manganese inhibits mitochondrial aconitase: a mechanism of manganese neurotoxicity. *Brain Res* 1998;799(2):334-342.

Figure 1: Distribution of past-3-months individual exposure levels across welders. The red line indicates the dividing line between welders with higher exposure (HEX) and lower exposure (LEX)

Figure 2: Thalamus a) and striatum b) VOI for GABA measurements shown on sagittal and AC-PC aligned views on T2-weighted images, and on an axial view of a brain tissue map (red: white matter, blue: grey matter, green: CSF). Please note the tissue maps have a slightly different angulation from the AC-PC aligned T2-weighted images. Also shown are typical GABA-edited spectra from thalamus (top) and striatum (bottom) fitted with LCModel (red lines).

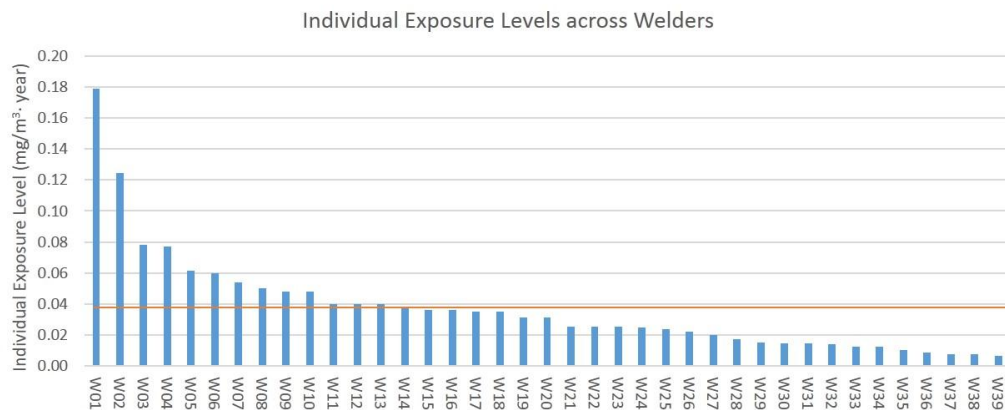
Figure 3. Regions of Interest (ROIs) of T1 value measurement in a) left and right globus pallidus (green) and caudate nucleus (cyan); b) left and right frontal cortex (blue); c) left and right substantia nigra (red).

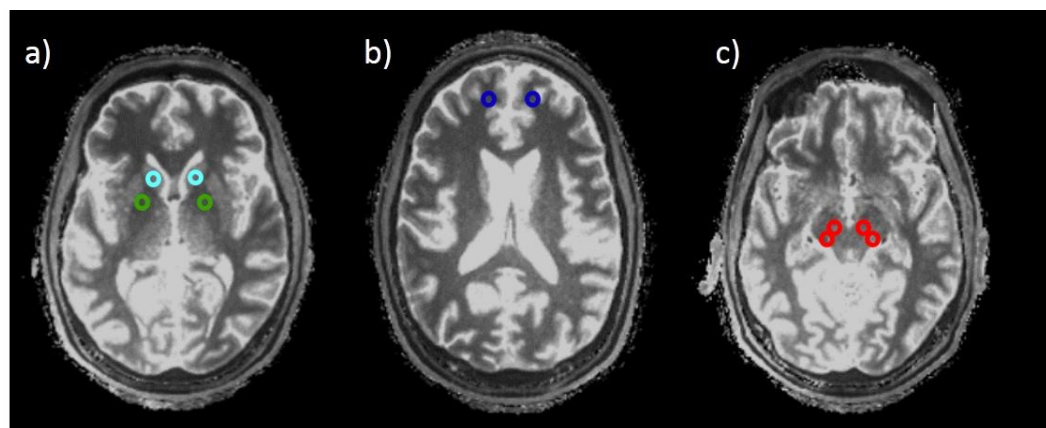
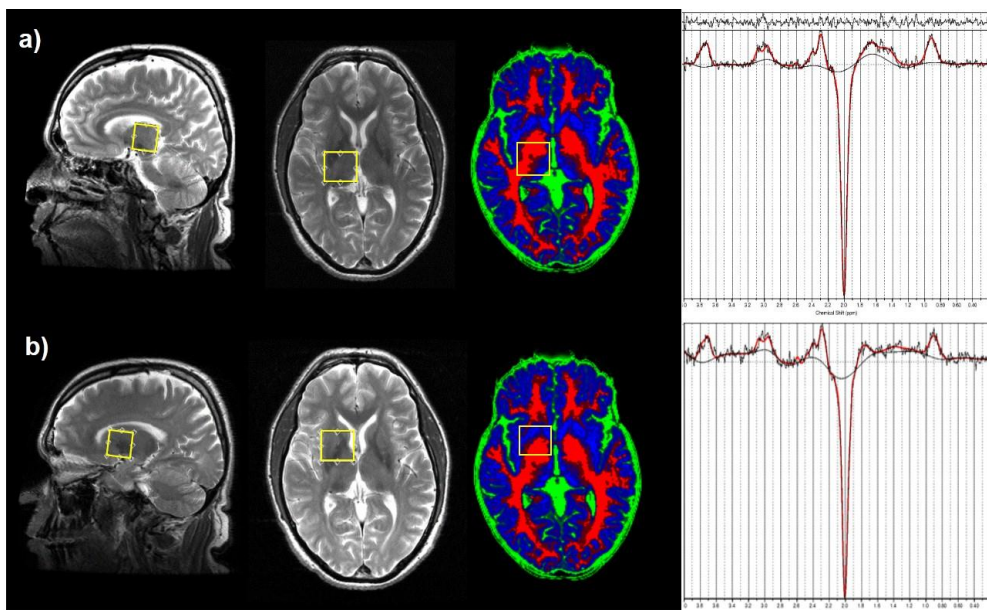
Figure 4. Example of T1 hyperintensity in the globus pallidus (GP) (red arrows) of a welder (left), compared to an unexposed control subject (right), displaying the mean R1 values from the GP for each subject.

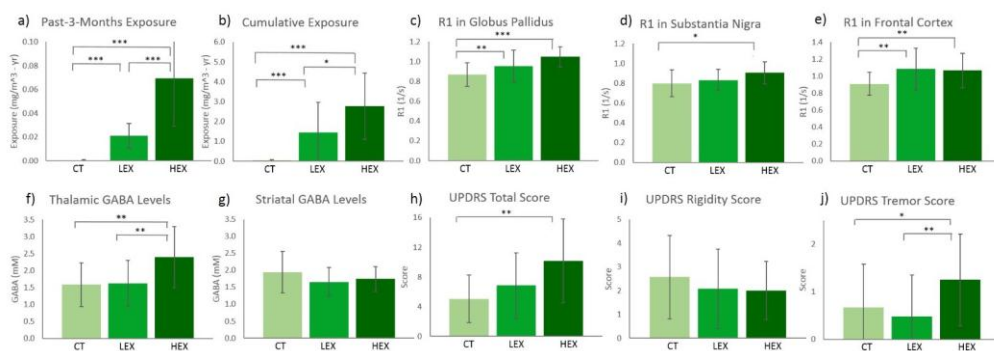
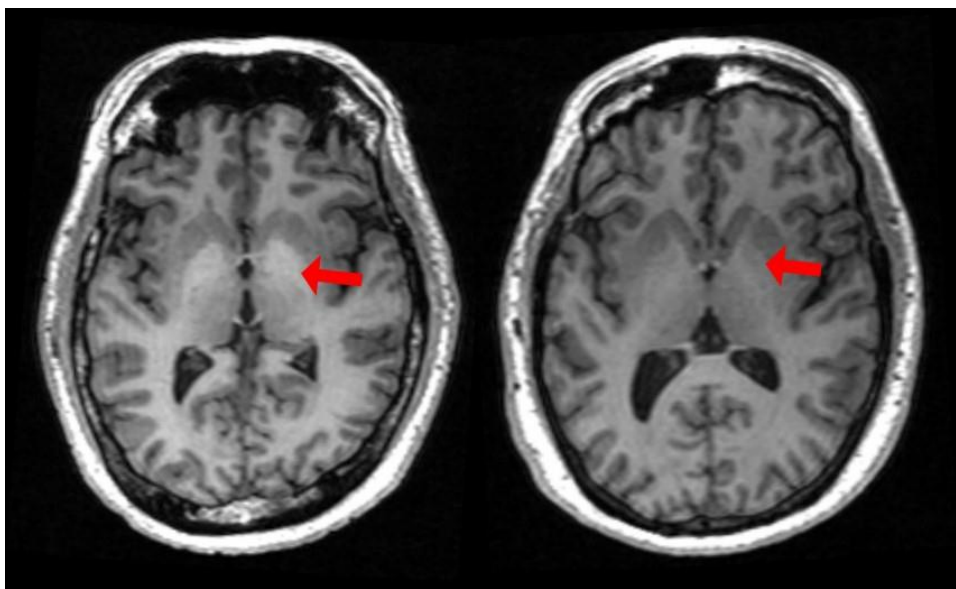
Figure 5. Group comparisons across controls (CT), welders with higher exposure (HEX) and with lower exposure (LEX): a) past-3-months and b) lifetime cumulative exposure levels; R1 values in c) the globus pallidus, d) substantia nigra and e) frontal cortex; f) thalamic and g) striatal GABA levels; h) UPDRS total score, i) UPDRS rigidity score and j) UPDRS tremor score; *, **, ***: p<0.05, p<0.01, p<0.001

Figure 6. Scatter plot of thalamic GABA levels vs. past-12-months exposure levels for all welders

Figure 7. Schematic diagram of basal ganglia-thalamo-cortical circuit. Blue, red and green arrows indicate dopaminergic, GABAergic and glutamatergic projections respectively. SNC: substantia nigra pars compacta, SNr: substantia nigra pars reticulata, GPe: globus pallidus external, GPi: globus pallidus internal, STN: subthalamic nucleus, D1 and D2: dopamine receptors D1 and D2.







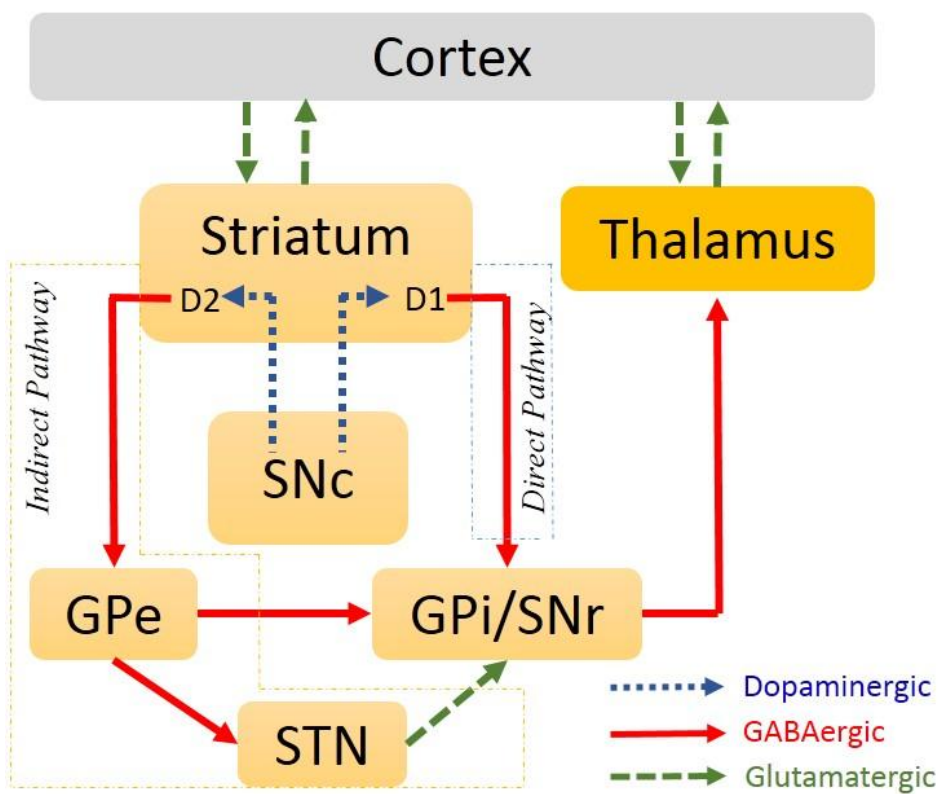
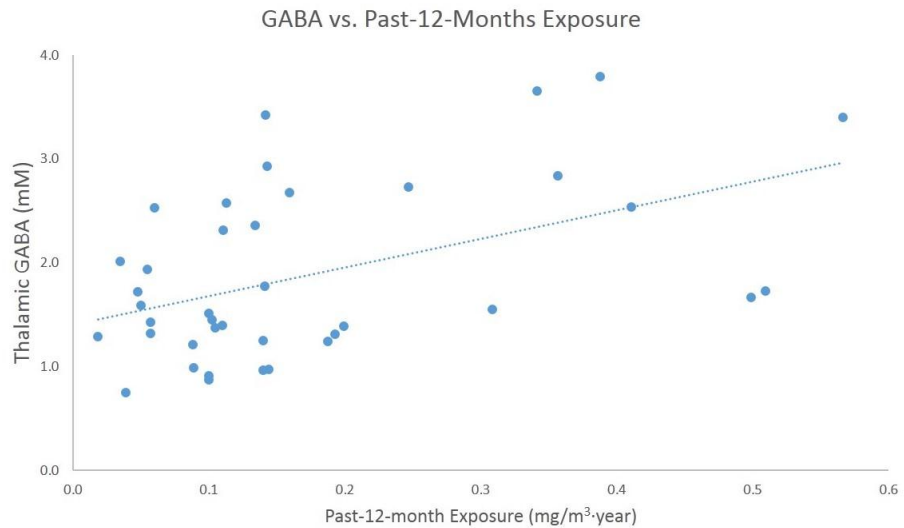


Table 1. Age, years of education, airborne respirable Mn, and mean years of Mn exposure for each group of the subjects, listed as mean (standard deviation)

	Controls	Welders	LEX Welders	HEX Welders
Number	22	39	26	13
Mean age	40 (12)	40 (11)	39 (11)	44 (10)
Mean years of education	13 (2)	13(2)	13 (2)	14 (2)
Mean airborne respirable Mn [mg/m ³]	0.002 (0.001)	0.17 (0.14)***	0.13 (0.10)***	0.23 (0.18)***,#
Mean years of exposure	0	12 (9)	11 (7)	16 (10)

***, p<0.001 for comparison between each Mn-exposed group and controls

, p<0.05 for comparison between welders with higher exposure (HEX) and lower exposure (LEX)

Table 2. Group comparisons of GABA levels, individual exposure levels with three exposure windows, R1 values and UPDRS scores with rigidity and tremor scores, listed as mean (standard deviation) for each group.

	Controls	Welders	LEX Welders	HEX Welders
Exposure levels ((mg/m ³)·yr)				
Past-3-Month	0.000 (0.000)	0.037 (0.033)***	0.021 (0.010)***	0.069 (0.040)***,###
Past-12-Month	0.002 (0.001)	0.174 (0.142)***	0.108 (0.090)***	0.307 (0.135)***,###
Cumulative	0.040 (0.035)	1.886 (1.664)***	1.448 (1.510)***	2.763 (1.665)***,#
GABA levels (mM)				
Thalamic GABA	1.563 (0.638)	1.881 (0.829)	1.624 (0.670)	2.395 (0.900)**,##
Striatal GABA	1.922 (0.606)	1.684 (0.403)	1.656 (0.422)	1.743 (0.370)
R1 values (1/s)				
Globus Pallidus	0.869 (0.096)	0.986 (0.154)**	0.955 (0.119)**	1.049 (0.198)***
Substantia Nigra	0.800 (0.136)	0.858 (0.124)	0.834 (0.128)	0.906 (0.102)*
Caudate Nucleus	0.704 (0.083)	0.764 (0.103)*	0.754 (0.106)	0.784 (0.096)*
Frontal Cortex	0.915 (0.136)	1.074 (0.225)**	1.078 (0.243)**	1.068 (0.192)**
UPDRS				
Total Score	5.0 (3.2)	7.9 (5.0)*	6.8 (4.4)	10.2 (5.7)**
Rigidity	2.6 (1.7)	2.1 (1.5)	2.1 (1.7)	2.0 (1.2)
Tremor	0.6 (0.9)	0.7 (1.0)	0.5 (0.9)	1.3 (0.9)*,##

* , **, *** p<0.05, p<0.01, p<0.001 for comparison to the control group

#,##,###, p<0.05, p<0.01, p<0.001 for comparison between welders with higher exposure (HEX) and lower exposure (LEX)

Table 3.1 Pearson correlations between GABA levels, exposure levels, brain R1 values and age, listed as correlation coefficients (*r*) and p values (*p*)

		GABA (Str)	Exp (P3M)	Exp (P12M)	Exp (CUM)	R1 (GP)	R1 (CN)	R1 (FT)	R1 (SN)	Age
GABA (Thal)	<i>r</i>	0.24	0.37	0.47	0.25	-0.03	0.05	0.34	0.51	0.21
	<i>p</i>	0.15	0.02	0.002	0.12	0.84	0.76	0.04	0.001	0.19
GABA (Str)	<i>r</i>		-0.003	0.14	0.09	0.13	0.11	0.56	0.341	0.16
	<i>p</i>		0.98	0.40	0.60	0.44	0.51	0.0003	0.04	0.34
Exp (P3M)	<i>r</i>			0.77	0.27	0.11	-0.03	-0.02	0.22	-0.05
	<i>p</i>			<0.0001	0.10	0.50	0.88	0.90	0.17	0.75
Exp (P12M)	<i>r</i>				0.29	0.04	-0.05	-0.05	0.25	0.02
	<i>p</i>				0.07	0.80	0.78	0.78	0.12	0.91
Exp (CUM)	<i>r</i>					0.07	-0.06	-0.01	0.12	0.43
	<i>p</i>					0.65	0.71	0.95	0.47	0.006
R1 (GP)	<i>r</i>						0.80	0.40	0.63	0.26
	<i>p</i>						<0.0001	0.01	<0.0001	0.11
R1 (CN)	<i>r</i>							0.54	0.66	-0.01
	<i>p</i>							0.0003	<0.0001	0.94
R1 (FT)	<i>r</i>								0.75	-0.12
	<i>p</i>								<0.0001	0.45
R1 (SN)	<i>r</i>									0.13
	<i>p</i>									0.42

GABA (Thal): thalamic GABA levels; GABA (Str): striatal GABA levels; Exp (P3M): past-3-month exposure levels; Exp (P12M): past-12-months exposure levels; Exp (CUM): cumulative exposure levels; R1 (GP): R1 values from the globus pallidus; R1(CN): R1 values from the caudate nucleus; R1 (FT): R1 values from the frontal cortex; R1 (SN): R1 values from the substantia nigra

Table 3.2 Pearson correlations between GABA levels, UPDRS total score, rigidity, tremor and age, listed as correlation coefficients (r) and p values (p)

		GABA (Str)	UPDRS	Rigidity	Tremor	Age
GABA (Thal)	r	0.24	0.16	0.22	0.15	0.21
	p	0.15	0.32	0.17	0.37	0.19
GABA (Str)	r		-0.02	-0.06	0.08	0.16
	p		0.92	0.72	0.63	0.34
UPDRS	r			0.50	0.61	0.45
	p			0.001	<0.0001	0.004
Rigidity	r				0.10	0.24
	p				0.55	0.15
Tremor	r					0.32
	p					0.05

GABA (Thal): thalamic GABA levels; GABA (Str): striatal GABA levels; UPDRS: UPDRS III total scores; Rigidity: Rigidity scores; Tremor: Tremor scores

Table 4.1 Type III SS analysis of each variable in the full model of regression on the thalamic GABA levels

Source	Type III SS	F Value	p Value
R1 (GP)	3.28	10.43	0.003
R1 (CN)	0.10	0.3	0.59
R1 (FT)	0.13	0.41	0.53
R1 (SN)	2.23	7.08	0.01
Age	1.54	4.92	0.03
Exp (P12M)	2.06	6.54	0.02
Exp (CUM)	0.0005	0.00	0.97

Table 4.2 Type III SS analysis of each variable in the full model of regression on the striatal GABA levels

Source	Type III SS	F Value	p Value
R1 (GP)	0.00002	0.00	0.99
R1 (CN)	0.03	0.27	0.61
R1 (FT)	2.03	20.14	0.0001
R1 (SN)	0.27	2.64	0.12
Age	0.51	5.11	0.03
Exp (P12M)	0.31	3.05	0.09
Exp (CUM)	0.06	0.61	0.44

Table 4.3 Results from the final model for regression analysis of the thalamic GABA levels on exposure levels and R1 values

Model Summary

df (model)	df (error)	Adj R-square	F value	p value
4	34	0.57	13.76	<0.0001

Coefficient Estimation

Variable	Parameter Estimation	t Value	p value	VIF	CI_upper	CI_lower
Exp (P12M)	1.72	2.66	0.01	1.10	3.03	0.41
R1 (GP)	-3.26	-4.28	0.0001	1.79	-1.71	-4.81
R1 (SN)	5.26	5.5	<0.0001	1.81	7.20	3.32
Age	0.02	2.39	0.02	1.08	0.037	0.003

Table 4.4 Results from the final model for regression analysis of the striatal GABA levels on exposure levels and R1 values

Model Summary

df (model)	df (error)	Adj R-square	F value	p value
4	32	0.48	7.46	0.0002

Coefficient Estimation

Variable	Parameter Estimation	t Value	p value	VIF	CI_upper	CI_lower
Exp (P12M)	0.89	1.96	0.06	1.33	1.81	-0.03
R1 (FT)	1.81	4.66	<0.0001	3.04	2.61	1.02
R1 (SN)	-1.80	-2.42	0.02	3.35	-0.28	-3.32
Age	0.01	2.5	0.02	1.16	0.02	0.002

Table 5.1 Type III SS analysis of each variable in the full model of regression on UPDRS total score

Source	Type III SS	F value	p Value
GABA (Thal)	11.08	0.49	0.49
GABA (Str)	11.05	0.49	0.49
Age	157.66	7.01	0.01

Table 5.2 Results from the final model for regression analysis of UPDRS total scores on GABA levels and age

<i>Model summary</i>					
df (model)	df (error)	Adj R-square	F value	p value	
1	37	0.18	9.44	0.004	
<i>Coefficient estimation</i>					
Variable	Parameter Estimation	t Value	p value	CI_upper	CI_lower
Age	0.21	3.07	0.004	0.35	0.07

Table 5.3 Type III SS analysis of each variable in the full model of regression on rigidity score

Source	Type III SS	F Value	p Value
GABA (Thal)	3.75	1.59	0.22
GABA (Str)	1.68	0.71	0.41
Age	2.96	1.25	0.27

Table 5.4 Type III SS analysis of each variable in the full model of regression on tremor score

Source	Type III SS	F Value	p Value
GABA (Thal)	0.03	0.03	0.86
GABA (Str)	0.02	0.02	0.89
Age	3.16	3.52	0.07

